Network patterns recognition for automatic dermatologic images classification

Costantino Grana[a], Vanini Daniele[a], Giovanni Pellacani[b], Stefania Seidenari[b], Rita Cucchiara[a]
[a]Department of Information Engineering
[b]Department of Dermatology
University of Modena, Via Vignolese 905/b, 41100 Modena, Italy

ABSTRACT

In this paper we focus on the problem of automatic classification of melanocytic lesions, aiming at identifying the presence of reticular patterns. The recognition of reticular lesions is an important step in the description of the pigmented network, in order to obtain meaningful diagnostic information. Parameters like color, size or symmetry could benefit from the knowledge of having a reticular or non-reticular lesion. The detection of network patterns is performed with a three-steps procedure. The first step is the localization of line points, by means of the line points detection algorithm, firstly described by Steger. The second step is the linking of such points into a line considering the direction of the line at its endpoints and the number of line points connected to these. Finally a third step discards the meshes which couldn't be closed at the end of the linking procedure and the ones characterized by anomalous values of area or circularity. The number of the valid meshes left and their area with respect to the whole area of the lesion are the inputs of a discriminant function which classifies the lesions into reticular and non-reticular. This approach was tested on two balanced (both sets are formed by 50 reticular and 50 non-reticular images) training and testing sets. We obtained above 86% correct classification of the reticular and non-reticular lesions on real skin images, with a specificity value never lower than 92%.

Keywords: pattern recognition, segmentation, dermoscopy, network pattern

1. INTRODUCTION

In this work, the problem of line detection, closure, thinning and images classification according to the presence of network patterns is addressed. Many natural images in fact contain network like structures, such as SAR landscapes, solar or medical images (heart physiology or dermatological conditions). This is a typical problem of non-uniform texture analysis, where edge detection cannot provide effective results by itself. Some approaches propose a global analysis of the textures in partitions of the image, such as with co-occurrence matrices, or wavelet transform, which characterize an area, but do not provide precise localization of the pattern within it [1]. A seminal work on linear structure identification is [2], which was applied on road detection and dermatological images [3].
In this paper, we will start from this important theoretical work, and address several open issues found in many actual cases, such as line threshold selection, closure on junction points and network features characterization in order to locate and quantify the network presence. The application is tested on dermatological melanocytic lesion images. A set of specific patterns have been described in literature, and clear significance of these structural characteristics (dots, dark globules and lesion network) has been observed [3]. The lesion network in particular is highly rated as a diagnostic parameter, especially if network line width and color and network distribution are taken into account.

2. LINE POINTS DETECTION

For line points detection we employ the approach described in [2], which works on gray level images. The image is regarded as a surface in which the pixel luminance value is the surface's height. In this perspective the lines are ridges and can thus be identified as those sets of points which satisfy at the same time two conditions on the first and on the second order derivatives computed in the direction orthogonal to the line. The first order derivative should be

zero, while the second order derivative should be characterized by a high module value. The direction of the line and its normal can be obtained from the matrix of second-order partial derivatives (i.e. the Hessian matrix):

$$H(x,y)=\begin{pmatrix} r_{xx} & r_{xy} \\ r_{xy} & r_{yy} \end{pmatrix} \tag{1}$$

where r_{xx}, r_{xy}, r_{yy} are the second order partial derivatives obtained convolving the image with bidimensional kernels which represent the discrete approximations of Gaussian continuous functions. The standard deviation of these functions, σ, is directly tied to the expected line width and, in particular, to the detection condition:

$$\sigma \geq w/\sqrt{3} \tag{2}$$

Such an inequality guarantees that the second derivative response has a single minimum in case of light lines on dark background and a single maximum in case of dark lines on light background, which is well defined in case of point in which the first derivatives is zero.
To determine if the first derivative in the direction orthogonal to the line has a zero point within the current pixel, we use a quadratic Taylor polynomial:

$$p(x)=r+r'x+\frac{1}{2}r''x^2 \tag{3}$$

where r, r' and r'' are the derivatives estimated by convolving the image respectively with the Gaussian kernel, the first order derivative and the second order derivative of the Gaussian kernel. This function provides an estimation of the behavior of the filtered image in the direction perpendicular to the line and allows, at the same time, the localization with subpixel precision of the line points. To obtain the exact zero solutions we need to find out all the points satisfying the condition $p'(x)=0$. Such points are given by the ratio:

$$x=-\frac{r'}{r''} \tag{4}$$

If we call (n_x,n_y) the vector with unity norm, pointing in the direction orthogonal to the line in the pixel with coordinates (x,y) and if we call $x=(p_x,p_y)$, with $(p_x,p_y)=(t\cdot n_x,t\cdot n_y)$, the previous equation may be rewritten as:

$$t=-\frac{r_x n_x+r_y n_y}{r_{xx}n_x^2+2r_{xy}n_x n_y+r_{yy}n_y^2} \tag{5}$$

Given a coordinate system centered in the current pixel, this is a line point if:

$$(p_x,p_y)\in\left[-\frac{1}{2},\frac{1}{2}\right]\times\left[-\frac{1}{2},\frac{1}{2}\right] \tag{6}$$

Of all the points satisfying the above condition, the significant ones are those in which the maximum module eigenvalue of the Hessian matrix is high. The discussion of the meaning of "high" is postponed to the next section.

3. DETECTED LINE POINTS SELECTION

The threshold on the maximum eigenvalue cannot be defined a priori for all the images we mean to analyze. In fact the eigenvalues vary from image to image according to the luminance mean and to the local contrast values. That's why we need an automatic method to select the eigenvalue threshold suitable for every image.
The first problem coincides with the choice of the points to consider for the application of the method. In fact the maximum eigenvalue at each point may be either positive or negative, corresponding respectively to dark curvilinear structures on a bright background or vice versa. Even if the line detection algorithm takes in account only points associated to positive eigenvalues, the assumption that in a lesion with network pattern the negative eigenvalues could present minima of the same magnitude of the positive ones could lead to the conclusion that even negative

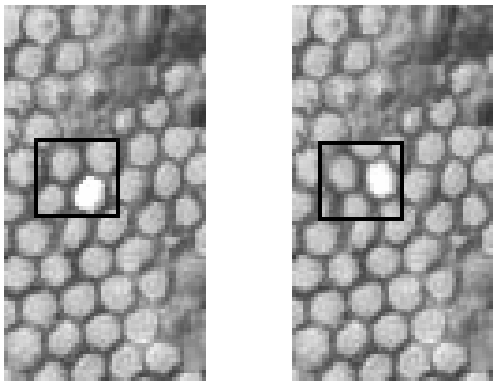

Fig. 1. Surrounding points rotation according to the local line direction. It is possible to see that the whole patch is now vertically aligned with the line it refers to.

values should be considered in our analysis. This is due to the fact that curvilinear structures found in the mash have comparable intensity to the network lines which surround it. Considering more points and having, in this way, a larger data set could positively influence the threshold selection process. Unfortunately experimental results showed like the above assumption is not true. That's why we decided to consider just the positive eigenvalues and in particular the positive eigenvalues computed in correspondence of lesion points and satisfying the condition (5).
The automatic selection process for the eigenvalue threshold is provided by the Fisher linear discriminant analysis [4]. The Fisher technique, analyzing the set of eigenvalues previously defined, identifies the threshold value λ_{th} which, maximizing the ratio between the interclass and intraclass dispersion, allows to divide the set of values into two well separated classes: the first of the points belonging to salient lines, the second of ones forming not so well defined linear structure. The interclass dispersion is given by the squared difference between the two classes averages, the intraclass dispersion by the sum of the two classes variances, so the value to be maximized is:

$$J(i) = \frac{\left|a_1(i) - a_2(i)\right|^2}{s_1^2(i) - s_2^2(i)}, i = 1 \ldots n \tag{7}$$

where $a_1(i)$ and $a_2(i)$ are the two class averages and $s_1^2(i)$ and $s_2^2(i)$ are the corresponding variances.

4. EIGENVALUES EQUALIZATION

Tests on a remarkable number of images showed that the algorithm selects not only the true line points, but even sets of points which normally wouldn't be classified as elements/parts of linear structures. These coincide with those points characterized by a high contrast, but only respect to one of the two regions defined by theirs surroundings. The selection mistake is due to the fact that the Gaussian filters are implemented with symmetrical convolution kernels. Such kernels weight indifferently the contributions given by the right and by the left side of the point.
Our solution to the problem, for every likely line point satisfying the condition (6) and characterized by a positive maximum eigenvalue, considers the surrounding points belonging to an hypothetical region whose size depends on the expected line width and oriented according to the local line direction. If the difference between the grey levels mean value of the right side and of the left side is greater than a fixed threshold, then the maximum eigenvalue in that point is scaled by a factor proportional to the difference of the two means.
The oriented set of surrounding pixels of the point (x, y) is obtained applying a rotation of an angle given by the local line direction and centered in the same point. As we work with matrix images and so as we work with discrete numbers, the new grey levels belonging to the oriented set of surrounding pixels are calculated by bilinear interpolation of the original grey levels close to the point.

$$\tilde{x} = x + i\cos\alpha - j\sin\alpha \tag{8}$$

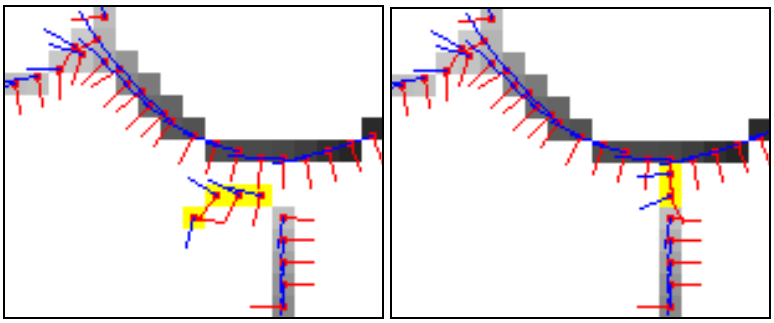

Fig. 2. Error in line closing and morphological correction.

$$\tilde{y} = y + i\sin\alpha + j\cos\alpha \tag{9}$$

where i and j vary from 0 to a value which depends on the expected line width and where α is the direction of the perpendicular to the line in the point (x, y). The grey level of the new pixel $(\tilde{x}, \tilde{y})$ is calculated by bilinear interpolation as the two new coordinates given by the expressions (8) and (9) are not integer but real. An example of this operation is shown in Fig. 1.

5. LINE CLOSURE

The set of line points obtained with the algorithm described above is neither complete nor closed: a closing process is needed. In [2], in order to close the lines, Steger proposes the use of some of the information already available from the previous steps, such as the perpendicular direction $(n_x, n_y) = (\cos\alpha, \sin\alpha)$, the line strength (second order derivative along α), and the subpixel localization of the line points (p_x, p_y). For each extreme point, the method look for a 3-point oriented neighborhood to minimize the sum $d + \beta$, where:

$$d = \|p_2 - p_1\|_2 \tag{10}$$

$$\beta = |\alpha_2 - \alpha_1|, \beta \in \left[0, \frac{\pi}{2}\right] \tag{11}$$

represent respectively the distance between the two points and the angular direction between the straights orthogonal to the line in the considered points. Unfortunately, this approach, which seems promising with ideal images, does not cope with the main problem in junction points, which are all those points in which one of the previous conditions are not satisfied: the direction deviates from the real line.

In particular, at junction points the weaker line (the line characterized by the lower contrast) gets parallel to the stronger one. In this case the algorithm often follows the stronger line failing to close the gap, even in case of small distances, producing parallel extensions of the lines. An example of this error is shown in Fig. 2.

Our solution begins with a first operation which, thanks to morphological masking, finds all the line terminations. To do this we employ a set of masks, such as those in Fig. 3. These masks are then rotated in the other three directions, in order to run out all these kind of terminations.

Every termination is characterized by a weighting factor, determined by the number of line pixels connected to it. This weight controls the amount of extension allowable for that termination. The extension is done in the direction of the line, as identified by the Hessian matrix, and is implemented at pixel level using the Bresenham algorithm [5]. If this extension is within the lesion boundaries and reaches another network element, it is confirmed and added to the network. Whether the extension grows in a direction which is parallel to the network segment being extended (wrong direction), or the extension doesn't reach any other network element within the maximum allowed extension, it is removed. Fig. 2 shows an example of correct extension.

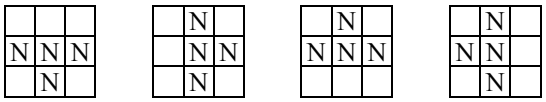

Fig. 4. Morphological masks for network thinning at “T” points.

6. EXTREME POINTS PRESERVING LINE THINNING

While in theory the line detection approach should provide single response, this was not observed in dermatological images, mainly because of the low contrast of the network and the discretization of the Gaussian kernels. So we introduced a one-pass raster thinning approach, which preserves the terminations. These are actually important for the diagnostic process, since they may point out the presence of abnormal lesion growth.
The thinning approach works by selectively eroding line points which match with exactly only one of the morphological masks of Fig. 4. These check for the presence of an “L” shaped point which is not an 8-connection between two different network segments. “T” shaped connections are then eroded with another set of masks (Fig. 4). This morphological filter is not well-behaved with respect to the line position, i.e. it moves the line to the rightmost position on every line, but this is not a problem for our application, since it is very uncommon to obtain lines which are wider than two pixels. For these lines in fact a position error is unavoidable, without going at sub-pixel level.

7. NETWORK POINTS VALIDATION

The main aim of our work is the automatic classification of skin lesions according to the presence or to the absence of network patterns. The statistical approach we used to classify the samples of the two classes is the linear discriminant analysis. This is primarily used to determine which variables discriminate between the two defined groups. We made a set of hypothesis about the more eligible variables and than verified the accuracy of our hypothesis running linear discriminant analysis and leave-one-out cross-validation on a set made up by 100 images. The variables for which we tested the discriminant power are the number of meshes, the percentage of reticular lesion, calculated as ratio between the area covered by the meshes and the whole area of the lesion, the percentage of reticular lesion, computed as ratio between the number of the pixels belonging to the network and the number of pixels of the lesion, a network compactness index, computed hence the information given by the relative positions of the meshes and a series of variables characterizing the texture of the image (variables like energy, entropy, contrast and uniformity). Experimental results showed that the most meaningful parameters, that is the parameters characterized by the highest discriminant power are the number of meshes and the percentage of reticular lesion. Such variables are not computed directly hence the results of the previous steps. The network returned by the line detection and by the linking algorithms must be validate. The validation process extracts only the “good” closed meshes. The meaning of “good” will be explained soon. For the moment it’s enough to consider that the two algorithms don’t work perfectly, but introduce an usually small number of errors. The line detection algorithm doesn’t select only points belonging to the network but also pixel belonging to areas characterized by a high local contrast. Otherwise the linking algorithm sometimes causes the closure of meshes in reality opened.
The localization of closed meshes is done thanks to labeling and erosion procedures. The validation process is something more complex as it depends on a series of parameters like perimeter, area and circularity of the meshes and number of perimeter points added by the linking algorithm. In particular the area of the mesh will have to be included in a gap determined by the expected line width. For instance, the computation of the minimum area

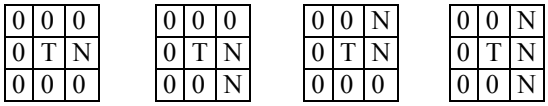

Fig. 3. Morphological masks for network terminations search. T is the termination point, while N is a network point.

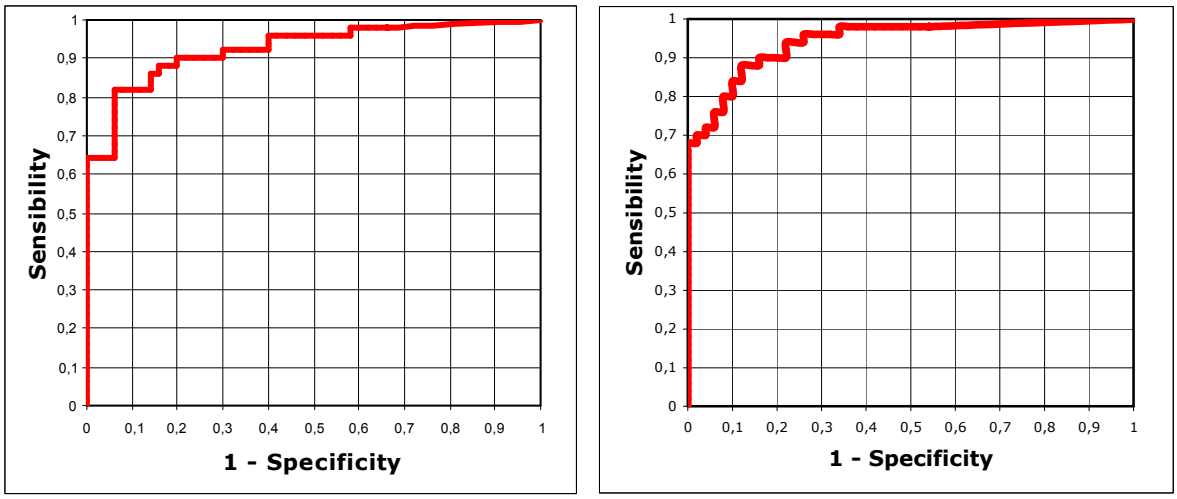

Figure 5. ROC curve on the training set (left) and on the test set (right).

(corresponding to the smallest possible mesh) is based on the consideration that the area of smallest mesh, if w is the expected width, will be given by:

$$A_{\min} = \pi w^2 \tag{12}$$

The circularity of the mesh, on the other side, computed as weighted ratio between the area A and the perimeter p of the mesh, according to the expression:

$$c = \frac{4\pi A}{p^2} \tag{13}$$

will have to be higher than a threshold reasonably fixed. Finally, the percentage of perimeter points added by the linking algorithm for the current mesh will have to be lower than a percentage computed keeping as reference the total number of pixels forming the perimeter of the mesh.

8. CLASSIFICATION RESULTS

To test the ability of the algorithm in the classification of skin lesion images according to the presence of network patterns, a set of 200 selected lesions was examined and divided into two classes (100 lesions per class) by the dermatologists. The first class includes lesions characterized by no network pattern, while the second one includes the lesions in which the network pattern is present both completely and partially. All the images were captured by a single instrument (FotoFinder® Dermoscope II), at the same resolution of 767x576 pixels and at a fixed zoom of 20x.

The original set of 200 images was split into two smaller sets so that each new set was formed by 50 reticular lesions and 50 non-reticular lesions. The first one was used to train the classifier that is to select the variables for the analysis and to compute the linear discriminant coefficients, while the second one was used to really test the effectiveness of the method. In the future we will simply refer to the two sets by using respectively the terms "training set" and "test set". The results are summarized in the Table 1 and in the ROC curve graphs (Fig. 5).

From Table 1, it follows a specificity of the 94%, a sensibility of the 82% and an effectiveness of the 88% for the training set and a specificity, a sensibility and an effectiveness, respectively, of the 94%, of the 72% and of the 83% for the test set.

If we try to invert the training set and the test set, to figure out if the good results are influenced by the particular choice of the two sets, the specificity, the sensibility and the effectiveness don't get worst. In particular the values for the specificity, the sensibility and the effectiveness for the training set are 92%, 76% and 84% while for the test set the values of the same parameters are 94%, 82% and 88%.

Table 1. Results on the training (left) and on the test set (right).

	Non-Reticular	Reticular
Non-Reticular	47	3
Reticular	9	41

	Non-Reticular	Reticular
Non-Reticular	47	3
Reticular	14	36

From the point of view of the dermatologists, the one to be optimized coincides with the specificity: it's acceptable to lose some reticular lesions, but it is desirable not to misclassify lesions in which the reticular pattern is not present. For this reason we tried to minimize the number of false positives. These are generated by images affected by noise. Noise which can be caused by the presence of hairs or air bubbles or simply by the presence of dust on the instrument lens during the capturing process. Besides these typologies of not ideal images there is a more difficult to manage class of noisy lesions: the ones in which an inverse network pattern is present. In this case the closeness of light linear structures generates a not existing dark network (Fig. 7). The following picture, differently, shows an example of consistent identification and localization of a true network.

9. CONCLUSIONS

A full lesion classification on the basis of the network pattern was described, which is able to cope with low contrast network patterns, does not need threshold selection, correctly closes different contrast meshes and produces 8-connected one-pixel wide network lines.

REFERENCES

1. M. Anantha, R.H. Moss , W.V. Stoecker, Detection of pigment network in dermatoscopy images using texture analysis, Comput Med Imaging Graph, 28(5):225–34, 2004.
2. C. Steger. An unbiased detector of curvilinear structures. IEEE Trans Pattern Anal Machine Intell, 20(2), Feb. 1998.
3. M. G. Fleming, C. Steger, J. Zhang, J. Gao, A. B. Cognetta, I. Pollak, and C. R. Dyer. Techniques for a structural analysis of dermatoscopic imagery. Comput Med Imaging Graph, 22:375–389, 1998.
4. Y. Deng, S. Kenney, M. Moore, and B. S. Manjunath. Peer group filtering and perceptual color image quantization. In IEEE Int Symp Circuits Systems VLSI (ISCAS'99), volume 4, pages 21–24, Orlando, FL, June 1999.
5. J. E. Bresenham. Algorithm for computer control of a digital plotter. IBM Systems Journal, 4(1):25–30, 1965.

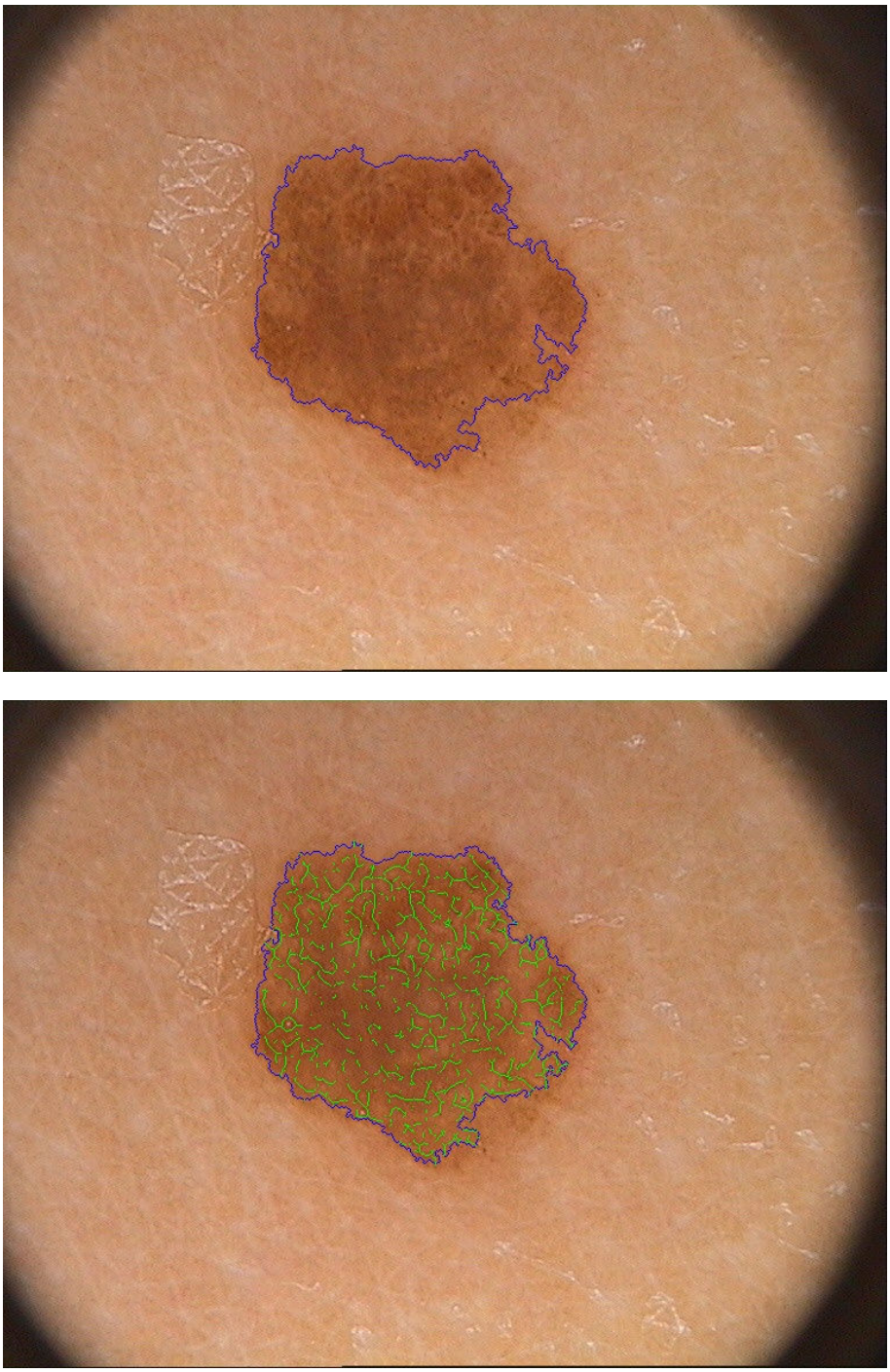

Figure 6. Example of false positive, showing how an inverse network deceives the algorithm.

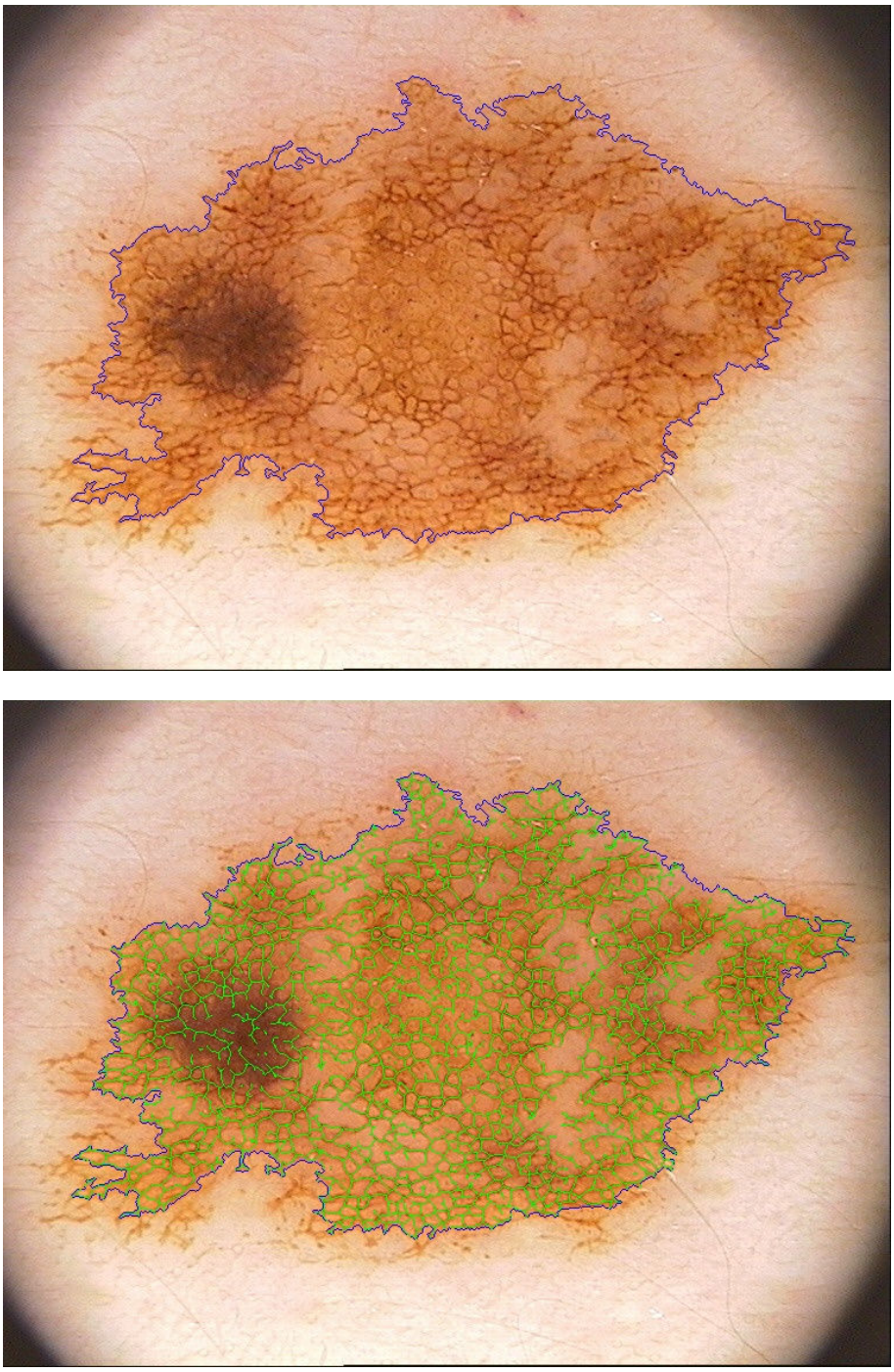

Figure 7. Example of a good identification and localization of the network.